ACS Macro Letters

pubs.acs.org/macroletters Letter

Sustainable and Recyclable Acrylate Resins for Liquid-Crystal Display 3D Printing Based on Lipoic Acid

Shiwei Han, Valentin A. Bobrin, Maxime Michelas, Craig J. Hawker,* and Cyrille Boyer*

Cite This: ACS Macro Lett. 2024, 13, 1495−1502 Read Online

ACCESS | Metrics & More | Article Recommendations | Supporting Information

ABSTRACT: The development of renewable vinyl-based photopolymer resins offers a promising solution to reducing the environmental impact associated with 3D printed materials. This study introduces a bifunctional lipoate cross-linker containing a dynamic disulfide bond, which is combined with acrylic monomers (*n*-butyl acrylate) and conventional photoinitiators to develop photopolymer resins that are compatible with commercial stereolithography 3D printing. The incorporation of disulfide bonds within the polymer network's backbone imparts the 3D printed objects with self-healing capabilities and complete degradability. Remarkably, the degraded resin can be fully recycled and reused for high-resolution reprinting of complex structures while preserving mechanical properties that are comparable to the original material. This proof-of-concept study not only presents a sustainable strategy for advancing acrylate-based 3D printing materials, but also introduces a novel approach for fabricating fully recyclable 3D-printed structures. This method paves the way for reducing the environmental impact while enhancing material reusability, offering significant potential for the development of eco-friendly additive manufacturing.

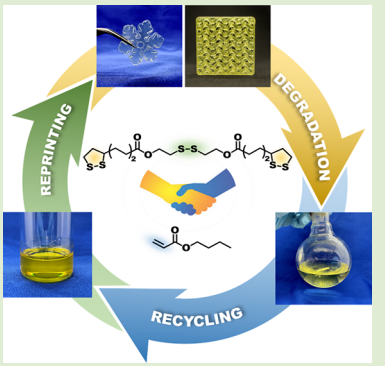

Additive manufacturing, commonly known as 3D printing, is revolutionizing the fabrication of intricate 3D structures across various industries, from rapid prototyping and customized medical implants to aerospace and automotive components.[1−4] Among the diverse techniques available, stereolithography techniques, including digital light processing (DLP) and liquid-crystal display (LCD), have gained significant traction due to their capabilities to produce complex designs with remarkable speed and precision.[5−7] These stereolithography techniques operate by selectively curing a liquid resin, composed of monomers and cross-linkers, layer by layer using light, ultimately forming durable, typically non-degradable, thermoset materials. However, unlike thermoplastics, these highly cross-linked materials are difficult to reprocess or recycled, contributing to the growing problem of plastic waste.[8] Additionally, the reliance on petrochemical-based vinyl monomers in this process further exacerbates environmental concerns. As 3D printing technology continues to advance, the ability to efficiently recycle materials at the end of their lifecycle will be essential for ensuring a sustainable future for this transformative industry, especially in light of upcoming European Union regulations mandating the use of fully recyclable materials by 2050 as part of the effort to achieve a circular economy.[9] Complying with these regulations will necessitate a significant shift in the development and adoption of sustainable 3D printing resins. Despite ongoing efforts, this research area remains dominated by acrylate-based photoresins due to their low cost, widespread availability, and rapid curing, which yield robust, highly cross-linked materials. However, these conventional acrylate resins are particularly problematic due to the formation of carbon−carbon backbone chains upon polymerization with the stability of the C−C bonds making them highly resistant to degradation and therefore difficult to recycle.

Recent research has investigated innovative approaches to overcome these limitations by incorporating reversible bonds, such as disulfide, imine, urea bonds, and others,[10−15] to construct dynamic exchange networks in materials.[16−18] One promising direction involves the use of lipoic acid (LA), a bioderived compound with a 1,2-dithiolane structure, which has been widely recognized for its applications in biomedicine and medical materials.[19−25] Recently, this material has regained attention for its potential in developing sustainable resins for DLP/LCD 3D printing. LA can undergo radical or thiolate initiated ring-opening polymerization to create materials with degradable properties.[26−34] Albanese et al. have demonstrated that thiyl radicals generated by LA during radical-initiated ROP could effectively undergo copolymerization with commodity vinyl monomers, incorporating degradable S−S units into the backbone of vinyl polymers.[35−37] Dual-cross-linking resins could also be developed by combining LA-functionalized macromonomers with acrylate cross-linkers,

Received: September 2, 2024
Revised: October 15, 2024
Accepted: October 18, 2024
Published: October 24, 2024

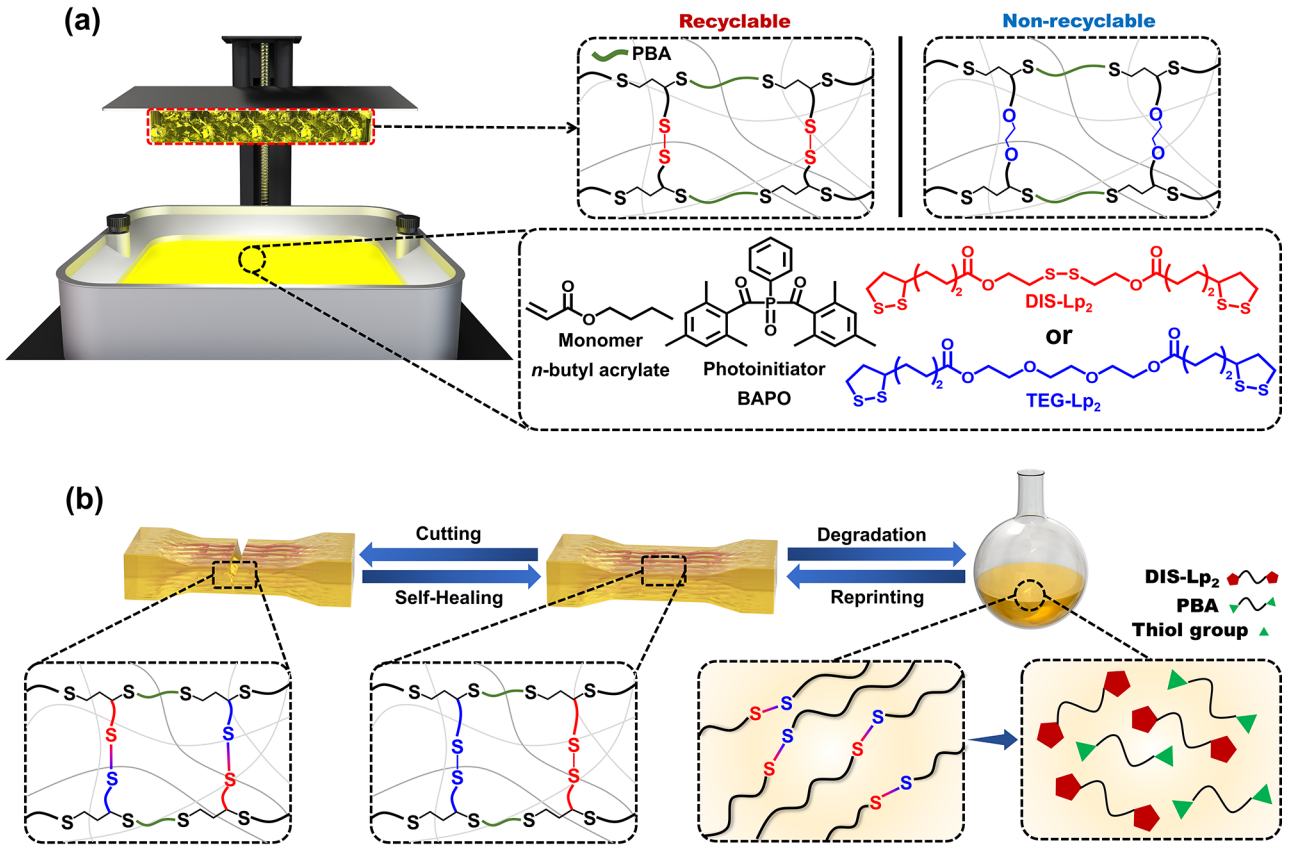

Figure 1. (a) Chemical structures of resin components, including *n*-butyl acrylate, DIS-Lp_2/TEG-Lp_2 cross-linkers and photoinitiator (BAPO) used in the LCD 3D printer and their resulting networks. (b) Schematic of the self-healing, degradation, and recycling of the printing material by using DIS-Lp_2 as a cross-linker.

resulting in a network with self-healing properties due to the presence of dynamic disulfide bonds, which were activated under a strong base (1,8-diazabicyclo[5.4.0] undec-7-ene (DBU)).[38] However, the high-cross-link density of these systems limited their degradability and the recovery/recycling of the resins following attempted degradation was not investigated. Blasco et al. described the preparation of a double network using LA and two vinyl monomers (4-acryloylmorpholine (ACMO) and 1-vinyl-2-pyrrolidone (NVP)) through a two-step process, including a photocuring followed by a thermal treatment.[39] This thermoplastic material exhibits customizable mechanical properties and could be recycled through multiple pathways, including reprinting. However, the lower thermal stability of thermoplastics compared to thermosets may limit their potential application in high-temperature environments. More recently, Dove's group explored multifunctional LA derivatives to develop a series of LA-based photoresins.[40] By using 1,2-dithiolane-functional monomers in place of traditional vinyl systems for polymerization, they produced cross-linked materials through DLP 3D printing that could be depolymerized and reprinted. Based on these advancements, the further development of renewable acrylate-based photoresins is an attractive target that would expand the performance and properties of recyclable resins for 3D printing.

Inspired by these seminal studies, we decided to develop a fully recoverable acrylic-based resin suitable for LCD 3D printing. To achieve this aim, we synthesized a difunctional lipoate cross-linker (Lp_2), featuring two lipoate units connected by a degradable disulfide linker. As a cross-linker, Lp_2 could then be formulated with *n*-butyl acrylate (BA) as a model monomer and a photoinitiator to prepare photoresins. These resins, with BA/Lp_2 weight (wt) ratios ranging from 50:50 wt % to 10:90 wt % (molar ratios ranging from approximately 81/19 mol % to 32/68 mol %), proved capable of printing high-resolution complex objects. The resulting 3D printed cross-linked materials exhibited self-healing properties, with the networks able to reform in the presence of a small amount of DBU when heated at 60 °C for 1 h. Additionally, when immersed in a low-concentration DBU solution (0.05 M), the cross-linked materials fully degraded, enabling the recovered resins to be reused for reprinting geometrically complex structures. This development marks a significant advancement in creating 3D printed materials that are both functional and environmentally sustainable.

Herein, we synthesized two different cross-linkers containing multiple lipoate groups to investigate their effects on the degradability and self-healing properties of the resulting polymer networks. From biorenewable and readily available LA, reaction with either 2-hydroxyethyl disulfide or triethylene glycol via an 1-ethyl-3-(3-(dimethylamino)propyl)-carbodiimide (EDC)/4-dimethylaminopyridine (DMAP) coupling reaction, yielding two distinct cross-linkers: one containing a disulfide bond (denoted DIS-Lp_2, Figure 1a, SI, Scheme S1) and the other with a nondynamic ethylene glycol unit (denoted TEG-Lp_2, Figure 1a, SI, Scheme S2). ^{1}H NMR spectroscopy and size exclusion chromatography (SEC) analysis confirms the successful synthesis of these two

https://doi.org/10.1021/acsmacrolett.4c00600
ACS Macro Lett. 2024, 13, 1495−1502

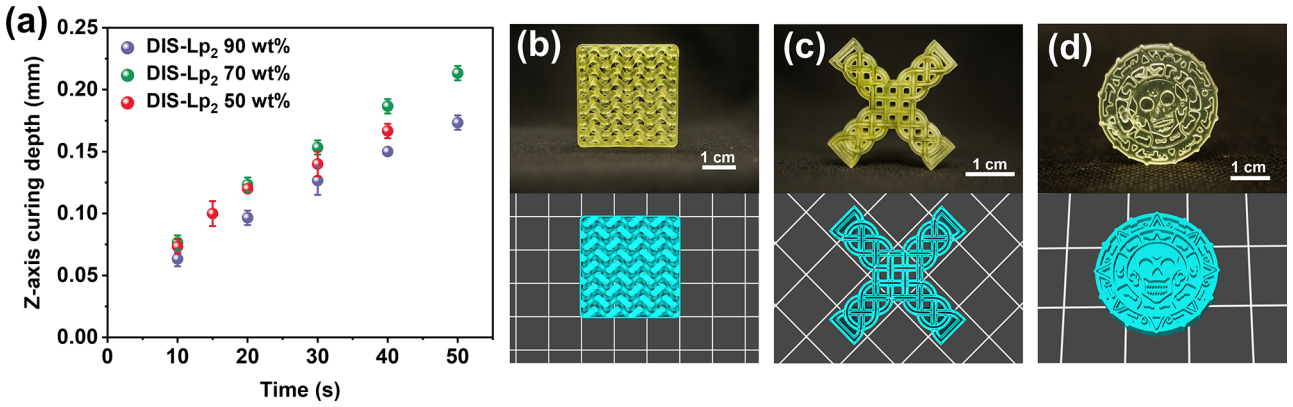

Figure 2. (a) Curing depth tests and printing of complex 3D objects using various BA/DIS-Lp$_2$ formulations: (b) 10/90 wt %, (c) 30/70 wt %, and (d) 50/50 wt %.

Table 1. Comparison of Glass Transition Temperature (T_g), Storage Modulus (25 °C), Elongation, Young's Modulus, and Resilience of Printed Samples with Different Resin Formulations

resins formulations	T_g (°C)	storage modulus @ 25 °C (MPa)	elongation (%)	Young's modulus (MPa)	resilience (MJ·m^{-3})
BA/DIS-Lp$_2$ 10/90 wt %	4.61	13.025	19.24 ± 1.08	7.00 ± 0.21	0.15 ± 0.04
BA/DIS-Lp$_2$ 20/80 wt %	1.26	11.556	19.81 ± 1.08	6.26 ± 0.14	0.11 ± 0.02
BA/DIS-Lp$_2$ 30/70 wt %	0.40	10.426	19.05 ± 2.24	5.31 ± 0.15	0.10 ± 0.04
BA/DIS-Lp$_2$ 40/60 wt %	−1.62	11.128	20.81 ± 3.69	4.74 ± 0.14	0.10 ± 0.03
BA/DIS-Lp$_2$ 50/50 wt %	−5.75	6.078	20.81 ± 1.69	3.34 ± 0.07	0.07 ± 0.02
BA/TEG-Lp$_2$ 30/70 wt %	−10.49	9.556	16.14 ± 2.59	4.44 ± 0.16	0.05 ± 0.02

compounds (SI, Figures S1−S6). Subsequently, these cross-linkers were formulated with BA as the comonomer and phenylbis(2,4,6-trimethylbenzoyl)phosphine oxide (BAPO) as the photoinitiator to obtain photoresins (Figure 1a). BA was selected as the model monomer not only for its compatibility with other components, enabling solvent-free printing, but also for its rapid and efficient photopolymerization, which is well-suited for open-air 3D printing processes.[41−45] All objects were printed using a commercial LCD printer provided by Anycubic (λ_{max} = 405 nm and I_0 = 2 mW·cm^{-2}; SI, Figures S7).

3D printing: First, we conducted printability tests on various formulations of BA/DIS-Lp$_2$ photoresins to determine the printable window range for our formulated resins (SI, Figure S8 and Table S1). The results revealed that, at a fixed 30 s exposure time, successful 3D printing was only achieved when the resin contained at least 50 wt % DIS-Lp$_2$. Resins with less than 50 wt % DIS-Lp$_2$ produced printed samples that thinned out and failed to reach the desired layer thickness. Specifically, at 20 wt % DIS-Lp$_2$, the resin did not lead to any observable 3D printed objects, indicating that insufficient cross-linker was incorporated to create a strong network, leading to print failure. Subsequently, we selected three formulations with 90, 70, and 50 wt % DIS-Lp$_2$ for curing depth tests (Figure 2a). All three resins achieved the target layer thickness (0.1 mm) within 30 s, with the 70 wt % DIS-Lp$_2$ exhibiting a greater Z-axis curing depth compared to those with 90 wt % DIS-Lp$_2$, indicating that higher BA content enhances the resin's curing efficiency. At or below 50 wt % DIS-Lp$_2$, the printed samples became opaque with increasing layer thickness, significantly reducing light penetration and impairing the curing of upper layers (SI, Figure S8).

FTIR analysis revealed that the objects printed with the three formulations containing 90, 70, and 50 wt % DIS-Lp$_2$ achieved a very high BA conversion rate of over 98% within a 30-s exposure time (SI, Figure S9). In addition, the photopolymerization tracked by ^{1}H NMR in a diluted dichloromethane (DCM) solution of BA/DIS-Lp$_2$ 50/50 wt % also confirms the successful polymerization of DIS-Lp$_2$ and BA (Figure S10). Specifically, after polymerization, the signals at 3.1 and 3.5 ppm corresponding to the 1,2-dithiolane ring of DIS-Lp$_2$ decrease, and a new peak appears at 2.8 ppm, indicating successful ring-opening polymerization. Meanwhile, a characteristic broad peak at 4.0 ppm associated with the poly(*n*-butyl acrylate) (PBA) is also evident. Using this exposure time (30 s), we successfully printed three different complex objects (gyroid, cross, and coin, containing 90, 70, and 50 wt % of DIS-Lp$_2$, respectively) (Figure 2b−d). Each object exhibited high resolution, demonstrating that BA/DISLp$_2$ resin is fully compatible with our commercial LCD 3D printing. Moreover, DIS-Lp$_2$ is also compatible with other acrylate monomers, such as the biobased isobornyl acrylate (IBOA), enabling the formation of fully biobased products, which was demonstrated by the successful fabrication of high-resolution objects using three IBOA/DIS-Lp$_2$ resin formulations (SI, Figure S11).

To evaluate the mechanical performances of the 3D printed materials, we performed dynamic mechanical analysis (DMA) and tensile tests to determine their glass transition temperature (T_g), Young's modulus, and other mechanical properties. We observed that increasing the BA content in the resin resulted in a decrease in both T_g and Young's modulus (Table 1 and SI, Figure S12 and S13), allowing for the tuning of mechanical properties and making this novel resin become suitable not only for 3D printing but also for applications beyond it, such as soft robotics, adhesives, and wearable electronics.[46−49]

Self-healing: To perform self-healing experiments, we fixed the BA ratio at 30 wt % and tested both DIS-Lp$_2$ and TEG-Lp$_2$ cross-linkers. Before printing, curing depth and FTIR tests were also conducted on BA/TEG-Lp$_2$ resins, confirming that the same printing parameters were applicable. Complex 3D

https://doi.org/10.1021/acsmacrolett.4c00600
ACS Macro Lett. 2024, 13, 1495−1502

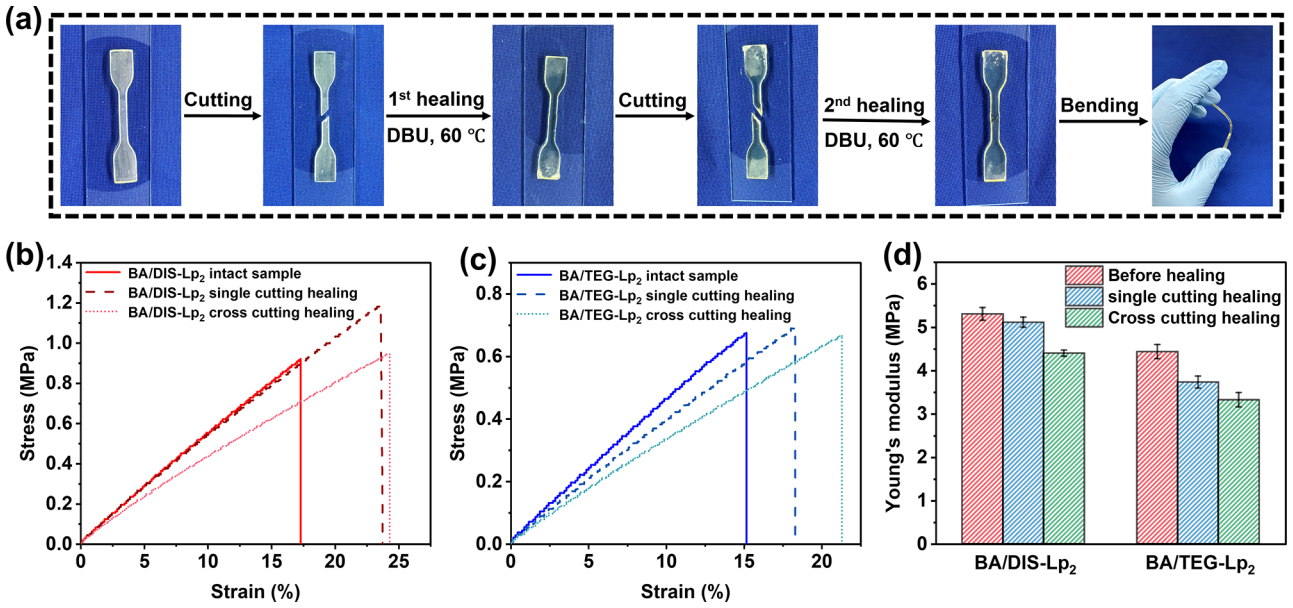

Figure 3. Self-healing results of 3D printed materials using DIS-Lp_2 or TEG-Lp_2: (a) Schematic representation of single-cut and double-cut healing processes. Stress−strain curves for (b) 30/70 wt % BA/DIS-Lp_2 samples and (c) 30/70 wt % BA/TEG-Lp_2 samples. (d) Comparison of Young's modulus before and after healing for samples printed with DIS-Lp_2 or TEG-Lp_2.

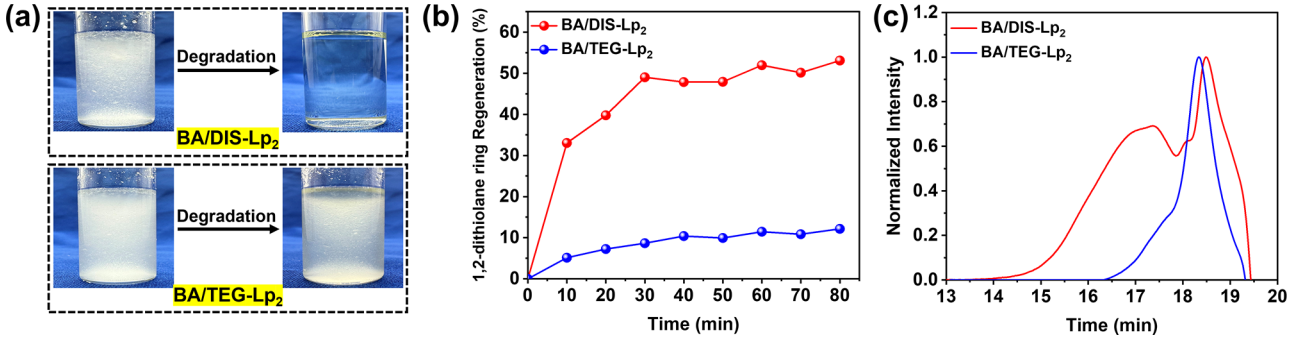

Figure 4. Degradation of materials printed with DIS-Lp_2 or TEG-Lp_2 (BA/Lp_2 = 30/70 wt %): (a) Photographs of samples before and after 2 h degradation in DBU solution (0.05 M, DCM) at room temperature. (b) Comparison of 1,2-dithiolane ring regeneration percentage over time and (c) SEC traces of dissolved polymers obtained after degradation of BA/DIS-Lp_2 or BA/TEG-Lp_2 networks, using THF as an eluent and PMMA calibration standards.

objects printed using a BA/TEG-Lp_2 30/70 wt % resin formulation exhibited high resolution, comparable to a BA/DIS-Lp_2 30/70 wt % formulation which allowed a range of equivalent tensile test samples to be 3D printed in a dumbbell shape using our established conditions (SI, Figures S15 and S16). As shown in Figures 3 and S17a, the samples were cut and then healed by applying DBU to the cut surfaces. The samples prepared using DIS-Lp_2 or TEG-Lp_2 exhibited complete self-healing within 1 h at 60 °C, as evidenced by the recovery of their mechanical properties. To verify the roles of DBU and the effect of temperature in promoting disulfide exchange and self-healing, two control experiments were conducted. First, to investigate the impact of temperature, samples treated with DBU at room temperature showed limited mechanical recovery within 1 h (SI, Figure S17b), with significantly reduced elongation in their stress−strain curves. Next, to examine the effect of DBU, samples were kept at 60 °C in the absence of DBU for extended periods, during which no healing was observed (SI, Figure S17a). For both cross-linkers, DMA results indicated no significant changes in the materials' rubbery plateau or T_g before and after self-healing (SI, Figure S18), suggesting that their cross-linking density was not substantially affected by the healing process. Encouraged by these successful results, we performed repeated cut-healing cycles to evaluate the impact of the dynamic disulfide linking group compared to the covalent ethylene glycol linker (Figure 3a). The stress−strain curves for BA/DIS-Lp_2 samples showed no significant change in Young's modulus after the first cut-healing cycle (Young's modulus decreased from 5.31 to 5.12 MPa, corresponding to a 3.6% decrease, SI, Table S3). However, a slight decrease in Young's modulus from 5.31 to 4.4 MPa (a 17.1% decrease) was observed after the second cycle (Figure 3b). This reduction is likely attributed to the introduction of defects during the cross-cutting process (SI, Figure S19), which negatively impacted the material's mechanical properties. In contrast, BA/TEG-Lp_2 samples showed a more pronounced reduction in Young's modulus after the healing cycles. The modulus decreased by 15.8% (from 4.44 to 3.74 MPa) after the first cycle, and further declined by 25% (from 4.44 to 3.33 MPa) after the second cycle (Figure 3d, SI, Table S3). These results demonstrate the impact of a higher density of disulfide bonds in BA/DIS-Lp_2

https://doi.org/10.1021/acsmacrolett.4c00600
ACS Macro Lett. 2024, 13, 1495−1502

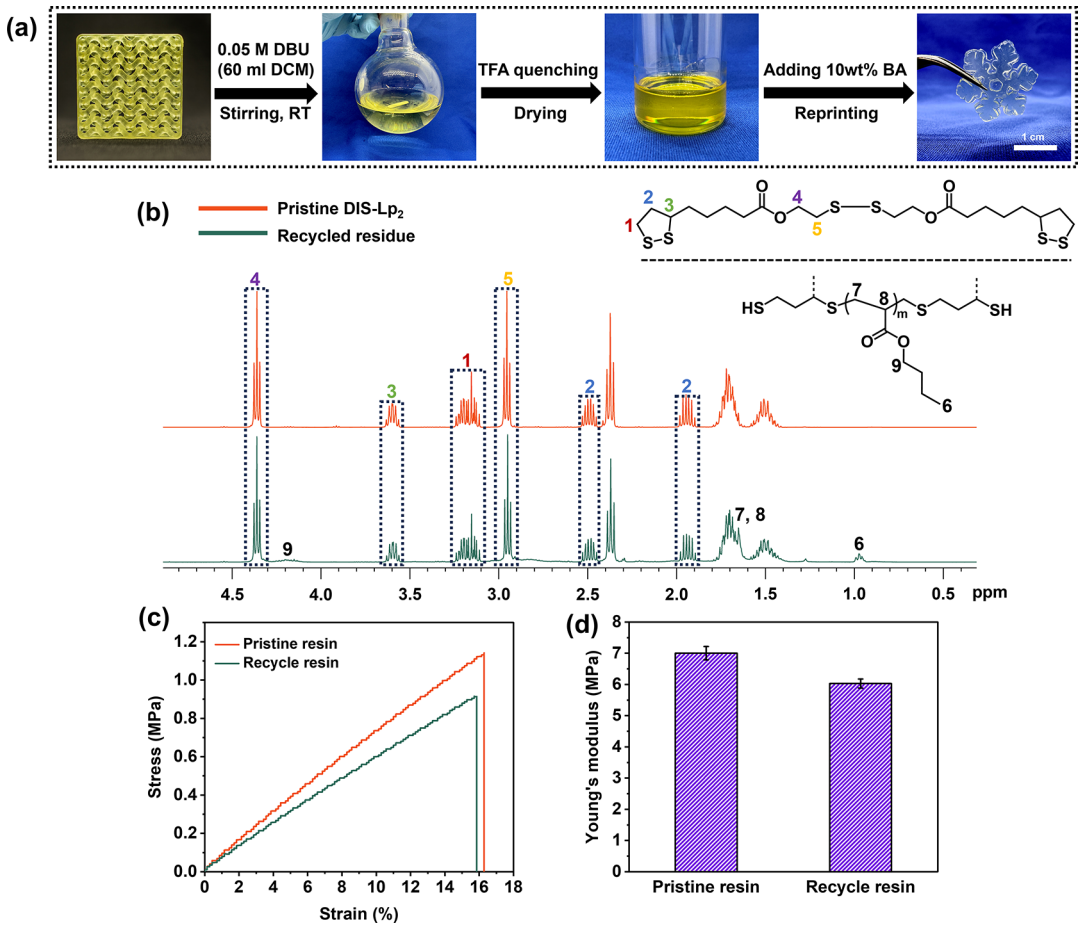

Figure 5. (a) Photographs illustrating the complete process of degrading, recycling, and reprinting a 3D printed object made from BA/DIS-Lp_2 10/90 wt % resin. (b) ^{1}H NMR spectra of DIS-Lp_2 and the recycled resin obtained after DBU treatment, demonstrating the chemical structure similarity and successful recovery of the resin. (c) Typical tensile test results for pristine samples and samples that have undergone degradation, recycling, and reprinting prepared using BA/DIS-Lp_2 10/90 wt % resin. (d) Average of Young's modulus of printing samples by using pristine resin (BA/DIS-Lp_2 10/90 wt %) and recycled resin (BA-recycle residue 10/90 wt %).

samples (backbone + cross-linkers) compared to BA/TEG-Lp_2 samples (backbone only) improve the self-healing capability of these materials.

Degradation study: Following successful 3D printing and self-healing, the degradability of these 3D printed materials prepared with either DIS-Lp_2 or TEG-Lp_2 was then investigated. Several catalyst systems were assessed for their ability to degrade BA/DIS-Lp_2 printed objects (SI, Table S4). Among these, only the DBU+DCM solution was selected, not just for its capacity to fully dissolve the samples, but more importantly, for its ability to recover DIS-Lp_2 cross-linker. Regarding the specific degradation process, Initially, samples based on 30 wt % BA were selected and grinded into a powder and then dispersed into a DCM solution containing 0.05 M DBU at room temperature. Significantly, the BA/DIS-Lp_2 samples completely dissolved within 2 h, resulting in a clear, pale-yellow solution with no residual solids. In contrast, BA/TEG-Lp_2 samples with 30 wt % BA were only partially soluble, even after 24 h. Additionally, the mass recovery percentage of soluble BA/DIS-Lp_2 derivatives was approximately 97%, whereas BA/TEG-Lp_2 samples exhibited a substantially lower recovery of soluble species (15.7%) (Figure 4a and SI, Figure S20). Furthermore, we tested other 3D printed objects based on different BA/DIS-Lp_2 formulations (BA content ranging from 10 wt % to 50 wt %), and all these materials were fully dissolved by treatment with DBU solution over 2 h at room temperature (SI, Figure S21).

To confirm that this process led to the reformation of the 1,2-dithiolane ring in lipoate derivatives, we monitored the reaction using UV−visible spectroscopy (SI, Figure S22). The 1,2-dithiolane ring exhibits a characteristic absorption peak at 335 nm. By measuring absorbance at different time points and applying the determined extinction coefficient of the 1,2-dithiolane ring (SI, Figure S23), we calculated the reformation of 1,2-dithiolane moieties over time (Figure 4b). Consistent with our degradation results, BA/TEG-Lp_2 samples displayed a significantly lower regeneration percentage compared to BA/DIS-Lp_2 samples. A plausible explanation for the high recovery of 1,2-dithiolane rings in the BA/DIS-Lp_2 system is that the central disulfide bonds within DIS-Lp_2 undergo dynamic exchange in the presence of DBU facilitating the disassembly of the network, and ultimately leading to the reformation of DIS-Lp_2 through a ring-closing reaction and formation of thiol-terminated PBA (Figure 1b).[35] This hypothesis is supported by SEC results (Figure 4c), which revealed a bimodal distribution for BA/DIS-Lp_2 samples. The narrow peak at around 19 min corresponds to the DIS-Lp_2 cross-linker, while the broader signal at a lower retention time is attributed to thiol-terminated PBA. Conversely, BA/TEG-Lp_2 samples display a single sharp signal corresponding to the TEG-Lp_2 cross-linker, with a minor

https://doi.org/10.1021/acsmacrolett.4c00600
ACS Macro Lett. 2024, 13, 1495−1502

amount of oligomer peaks, indicating that the network remained largely intact and undissolved.

Resin recovery and reprinting: Following our successful attempts to degrade 3D printed materials based on BA/DIS-Lp_2 resins, we assessed the feasibility of starting material recovery and reprinting. Based on ^{1}H NMR spectra and UV−vis spectra, we identified the 10/90 wt % BA/DIS-Lp_2 resin as the optimal composition for the reformation of 1,2-dithiolane rings (SI, Figures S24−S26 and Table S5). However, even with this optimized formulation, the recovery of the 1,2-dithiolane ring DIS-Lp_2 was limited to ∼65%. This limitation was attributed to the presence of BA connected to DIS-LP_2 (SI, Figure S27), as only adjacent DIS-LP_2 can effectively degrade and reform the 1,2-dithiolane ring (SI, Figure S27).[37] Additionally, SEC traces of the degradation products showed that, with only 10 wt % BA, the degraded residue contains only a small amount of short-chain PBA oligomers. As the BA content increases, the amount of PBA significantly increases, along with a broader distribution, indicating the formation of PBA polymers with increased degrees of polymerization (SI, Figure S28). In the first step of the recycling process, we degraded materials printed with BA/DIS-Lp_2 10/90 wt % using a 0.05 M DBU solution. After complete dissolution, a small amount of trifluoroacetic acid (TFA) was added to quench the DBU, preventing any residual DBU from causing recross-linking during resin recovery. After passing through a basic alumina column to remove excess TFA and then evaporating the solvent, the recovered resin was obtained as a yellow transparent oil (92.5% mass recovery percentage) with ^{1}H NMR spectroscopy showing primarily recycled DIS-Lp_2 (Figure 5a). Specifically, the characteristic peaks from the 1,2-dithiolane ring were observed. Significantly, only minor resonances at 0.8, 1.6, and 4.2 ppm corresponding to the CH_3, CH_2, and (CO)O−CH_2 of PBA oligomers were detected (Figure 5b).

Although the recovered resin can be directly cured through photopolymerization process (SI, Figure S29), its high viscosity prevented its direct use in DLP/LCD 3D printing. To prepare a printable recycled resin, an additional 10 wt % BA monomer (to reduce viscosity) and 1 wt % BAPO were added, ensuring the successful fabrication of high-resolution objects, such as the snowflake shown in Figure 5a. This result demonstrates the efficiency of the resin recovery process and the retention of high-fidelity performance. Tensile test specimens printed with the recycled resin were subjected to mechanical testing (SI, Figure S30), revealing a slight decrease, approximately 14%, in the mechanical properties compared to the pristine samples. However, these properties remained within an acceptable range (Figure 5c,d). In contrast, attempts to reconstitute viable resins from objects printed with BA/DIS-Lp_2 30/70 wt % resulted in a slight reduction in resolution and mechanical properties (SI, Figure S31), suggesting that the optimal BA content for maintaining high-resolution printing after recycling is crucial.

In summary, we have developed a recyclable resin system for LCD 3D printing that integrates acrylate monomers with a lipoic acid−based cross-linker featuring a central disulfide bond. The resulting 3D printing materials exhibited exceptional self-healing, degradability, showing promise for controlled life cycles by harnessing the dual functionality of dynamic disulfide bond exchange and lipoate-mediated reversible radical ring-opening polymerization with acrylate monomers. This study introduces a new paradigm for designing and fabricating degradable and recyclable acrylate-based materials, applicable not only to advanced 3D printing technology but also to industries such as self-healing coatings. This innovative approach enables the development of sustainable, multifunctional materials that address the increasing demand for environmentally conscious solutions in a variety of sectors.

■ ASSOCIATED CONTENT

Supporting Information

The Supporting Information is available free of charge at https://pubs.acs.org/doi/10.1021/acsmacrolett.4c00600.

Additional results, methods, materials, Figures S1−S24, and Table S1 (PDF)

■ AUTHOR INFORMATION

Corresponding Authors

Craig J. Hawker − *Department of Chemistry & Biochemistry and Materials Department, University of California, Santa Barbara, California 93106, United States;* orcid.org/0000-0001-9951-851X; Email: hawker@mrl.ucsb.edu

Cyrille Boyer − *Cluster for Advanced Macromolecular Design, School of Chemical Engineering, University of New South Wales, Sydney, NSW 2052, Australia; Australian Centre for Nanomedicine, School of Chemical Engineering, University of New South Wales, Sydney, NSW 2052, Australia;* orcid.org/0000-0002-4564-4702; Email: cboyer@unsw.edu.au

Authors

Shiwei Han − *Cluster for Advanced Macromolecular Design, School of Chemical Engineering, University of New South Wales, Sydney, NSW 2052, Australia*

Valentin A. Bobrin − *Cluster for Advanced Macromolecular Design, School of Chemical Engineering, University of New South Wales, Sydney, NSW 2052, Australia*

Maxime Michelas − *Cluster for Advanced Macromolecular Design, School of Chemical Engineering, University of New South Wales, Sydney, NSW 2052, Australia*

Complete contact information is available at: https://pubs.acs.org/10.1021/acsmacrolett.4c00600

Author Contributions

CRediT: **Shiwei Han** data curation, formal analysis, investigation, writing - original draft, writing - review & editing; **Valentin Bobrin** formal analysis, methodology, writing - review & editing; **Maxime Michelas** data curation, formal analysis, investigation, methodology, writing - review & editing; **Craig J. Hawker** investigation, supervision, writing - review & editing; **Cyrille Boyer** conceptualization, funding acquisition, supervision, writing - original draft, writing - review & editing.

Notes

The authors declare no competing financial interest.

■ ACKNOWLEDGMENTS

C.B. thanks the Australian Research Council for his Australian Laureate Fellowship (FL220100016). C.J.H. acknowledges support via the U.S. Army Research Office, Contract W911NF-19-D-0001, for the Institute for Collaborative Biotechnologies and the BioPACIFIC Materials Innovation Platform of the

National Science Foundation under Award No. DMR-1933487.

REFERENCES

(1) Truby, R. L.; Lewis, J. A. Printing soft matter in three dimensions. *Nature* **2016**, *540* (7633), 371−378.

(2) Gantenbein, S.; Masania, K.; Woigk, W.; Sesseg, J. P.; Tervoort, T. A.; Studart, A. R. Three-dimensional printing of hierarchical liquid-crystal-polymer structures. *Nature* **2018**, *561* (7722), 226−230.

(3) Kelly, B. E.; Bhattacharya, I.; Heidari, H.; Shusteff, M.; Spadaccini, C. M.; Taylor, H. K. Volumetric additive manufacturing via tomographic reconstruction. *Science* **2019**, *363* (6431), 1075−1079.

(4) Jung, K.; Corrigan, N.; Ciftci, M.; Xu, J.; Seo, S. E.; Hawker, C. J.; Boyer, C. Designing with Light: Advanced 2D, 3D, and 4D Materials. *Adv. Mater.* **2020**, *32* (18), 1903850.

(5) Walker, D. A.; Hedrick, J. L.; Mirkin, C. A. Rapid, large-volume, thermally controlled 3D printing using a mobile liquid interface. *Science* **2019**, *366* (6463), 360−364.

(6) Dong, M.; Han, Y.; Hao, X. P.; Yu, H. C.; Yin, J.; Du, M.; Zheng, Q.; Wu, Z. L. Digital Light Processing 3D Printing of Tough Supramolecular Hydrogels with Sophisticated Architectures as Impact-Absorption Elements. *Adv. Mater.* **2022**, *34* (34), 2204333.

(7) Quan, H.; Zhang, T.; Xu, H.; Luo, S.; Nie, J.; Zhu, X. Photo-curing 3D printing technique and its challenges. *Bioact. Mater.* **2020**, *5* (1), 110−115.

(8) Nyika, J.; Mwema, F. M.; Mahamood, R.; Akinlabi, E. T.; Jen, T. Advances in 3D printing materials processing-environmental impacts and alleviation measures. *Adv. Mater. Process.* **2022**, *8* (sup3), 1275−1285.

(9) How the EU wants to achieve a circular economy by 2050. Directorate General for Communication, European Parliament, 2024. https://www.europarl.europa.eu/topics/en/article/20210128STO96607/how-the-eu-wants-to-achieve-a-circular-economy-by-2050 (accessed 20 Aug 2024).

(10) Stouten, J.; Schnelting, G. H.; Hul, J.; Sijstermans, N.; Janssen, K.; Darikwa, T.; Ye, C.; Loos, K.; Voet, V. S.; Bernaerts, K. V. Biobased photopolymer Resin for 3D printing containing dynamic imine bonds for fast reprocessability. *ACS Appl. Mater. Interfaces* **2023**, *15* (22), 27110−27119.

(11) Vilanova-Pérez, A.; De la Flor, S.; Fernández-Francos, X.; Serra, À.; Roig, A. Biobased Imine Vitrimers Obtained by Photo and Thermal Curing Procedures − Promising Materials for 3D Printing. *ACS Appl. Polym. Mater.* **2024**, *6* (6), 3364−3372.

(12) Vilanova-Pérez, A.; Moradi, S.; Konuray, O.; Ramis, X.; Roig, A.; Fernández-Francos, X. Harnessing disulfide and transesterification bond exchange reactions for recyclable and reprocessable 3D-printed vitrimers. *React. Funct. Polym.* **2024**, *195*, 105825.

(13) Yang, L.; Sun, L.; Huang, H.; Zhu, W.; Wang, Y.; Wu, Z.; Neisiany, R. E.; Gu, S.; You, Z. Mechanically robust and room temperature self-healing ionogel based on ionic liquid inhibited reversible reaction of disulfide bonds. *Adv. Sci.* **2023**, *10* (20), 2207527.

(14) Zhu, G.; Zhang, J.; Huang, J.; Qiu, Y.; Liu, M.; Yu, J.; Liu, C.; Shang, Q.; Hu, Y.; Hu, L.; Zhou, Y. Recyclable and reprintable biobased photopolymers for digital light processing 3D printing. *Chem. Eng. J.* **2023**, *452*, 139401.

(15) Fang, Z.; Shi, Y.; Mu, H.; Lu, R.; Wu, J.; Xie, T. 3D printing of dynamic covalent polymer network with on-demand geometric and mechanical reprogrammability. *Nat. Commun.* **2023**, *14* (1), 1313.

(16) Wang, S.; Li, L.; Liu, Q.; Urban, M. W. Self-healable acrylic-based covalently adaptable networks. *Macromolecules* **2022**, *55* (11), 4703−4709.

(17) Wang, S.; Urban, M. W. Self-healing polymers. *Nature Reviews Materials* **2020**, *5* (8), 562−583.

(18) Yang, Y.; Urban, M. W. Self-healing polymeric materials. *Chem. Soc. Rev.* **2013**, *42* (17), 7446−7467.

(19) Zhang, Z.-Q.; Tong, P.-D.; Wang, L.; Qiu, Z.-H.; Li, J.-A.; Li, H.; Guan, S.-K.; Lin, C.-G.; Wang, H.-Y. One-step fabrication of self-healing poly (thioctic acid) coatings on ZE21B Mg alloys for enhancing corrosion resistance, anti-bacterial/oxidation, hemocompatibility and promoting re-endothelialization. *Chem. Eng. J.* **2023**, *451*, 139096.

(20) Mu, S.; Zhu, Y.; Wang, Y.; Qu, S.; Huang, Y.; Zheng, L.; Duan, S.; Yu, B.; Qin, M.; Xu, F. J. Cationic polysaccharide conjugates as antibiotic adjuvants resensitize multidrug-resistant bacteria and prevent resistance. *Adv. Mater.* **2022**, *34* (41), 2204065.

(21) Cui, C.; Mei, L.; Wang, D.; Jia, P.; Zhou, Q.; Liu, W. A self-stabilized and water-responsive deliverable coenzyme-based polymer binary elastomer adhesive patch for treating oral ulcer. *Nat. Commun.* **2023**, *14* (1), 7707.

(22) Zhu, Y.; Lin, M.; Hu, W.; Wang, J.; Zhang, Z. G.; Zhang, K.; Yu, B.; Xu, F. J. Controllable disulfide exchange polymerization of polyguanidine for effective biomedical applications by thiol-mediated uptake. *Angew. Chem.* **2022**, *134* (23), No. e202200535.

(23) Chai, C.; Guo, Y.; Huang, Z.; Zhang, Z.; Yang, S.; Li, W.; Zhao, Y.; Hao, J. Antiswelling and durable adhesion biodegradable hydrogels for tissue repairs and strain sensors. *Langmuir* **2020**, *36* (35), 10448−10459.

(24) Cui, C.; Sun, Y.; Nie, X.; Yang, X.; Wang, F.; Liu, W. A Coenzyme-Based Deep Eutectic Supramolecular Polymer Bioadhesive. *Adv. Funct. Mater.* **2023**, *33* (49), 2307543.

(25) Pal, S.; Shin, J.; DeFrates, K.; Arslan, M.; Dale, K.; Chen, H.; Ramirez, D.; Messersmith, P. B. Recyclable surgical, consumer, and industrial adhesives of poly (α-lipoic acid). *Science* **2024**, *385* (6711), 877−883.

(26) Albanese, K. R.; Read de Alaniz, J.; Hawker, C. J.; Bates, C. M. From health supplement to versatile monomer: Radical ring-opening polymerization and depolymerization of α-lipoic acid. *Polymer* **2024**, *304*, 127167.

(27) Choi, C.; Self, J. L.; Okayama, Y.; Levi, A. E.; Gerst, M.; Speros, J. C.; Hawker, C. J.; Read de Alaniz, J.; Bates, C. M. Light-mediated synthesis and reprocessing of dynamic bottlebrush elastomers under ambient conditions. *J. Am. Chem. Soc.* **2021**, *143* (26), 9866−9871.

(28) Zhang, Q.; Deng, Y.; Shi, C.-Y.; Feringa, B. L.; Tian, H.; Qu, D.-H. Dual closed-loop chemical recycling of synthetic polymers by intrinsically reconfigurable poly (disulfides). *Matter* **2021**, *4* (4), 1352−1364.

(29) Deng, Y.; Zhang, Q.; Qu, D. H.; Tian, H.; Feringa, B. L. A chemically recyclable crosslinked polymer network enabled by orthogonal dynamic covalent chemistry. *Angew. Chem.* **2022**, *134* (39), No. e202209100.

(30) Alraddadi, M. A.; Chiaradia, V.; Stubbs, C. J.; Worch, J. C.; Dove, A. P. Renewable and recyclable covalent adaptable networks based on bio-derived lipoic acid. *Polym. Chem.* **2021**, *12* (40), 5796−5802.

(31) Huang, J.; Wróblewska, A. A.; Steinkoenig, J.; Maes, S.; Du Prez, F. E. Assembling lipoic acid and nanoclay into nacre-mimetic nanocomposites. *Macromolecules* **2021**, *54* (10), 4658−4668.

(32) Levkovskyi, I. O.; Mochizuki, S.; Zheng, A.; Zhang, X.; Zhang, F. Lipoic acid-based poly (disulfide) s: Synthesis and biomedical applications. *Nano TransMed.* **2023**, *2*, 100006.

(33) Chen, M.; Yang, R.; Wu, H.; Wang, Q.; Shi, C.; Zhou, S. W.; Yang, D.; Liu, F. Y.; Tian, H.; Qu, D. H. Closed-Loop Recyclable Poly (ester-disulfide) s for Potential Alternatives to Engineering Plastic. *Angew. Chem., Int. Ed.* **2024**, *63* (38), e202409200.

(34) Lee, D.; Wang, H.; Jiang, S.; Verduzco, R. Versatile Light-Mediated Synthesis of Degradable Bottlebrush Polymers Using α-Lipoic Acid. *Angew. Chem., Int. Ed.* **2024**, na.

(35) Albanese, K. R.; Morris, P. T.; Read de Alaniz, J.; Bates, C. M.; Hawker, C. J. Controlled-Radical Polymerization of α-Lipoic Acid: A General Route to Degradable Vinyl Copolymers. *J. Am. Chem. Soc.* **2023**, *145* (41), 22728−22734.

(36) Albanese, K. R.; Morris, P. T.; Roehrich, B.; Read de Alaniz, J.; Hawker, C. J.; Bates, C. M. Selective electrochemical degradation of bottlebrush elastomers. *J. Polym. Sci.* **2024**, *62* (18), 4326−4331.

(37) Albanese, K. R.; Okayama, Y.; Morris, P. T.; Gerst, M.; Gupta, R.; Speros, J. C.; Hawker, C. J.; Choi, C.; de Alaniz, J. R.; Bates, C. M.

https://doi.org/10.1021/acsmacrolett.4c00600
ACS Macro Lett. 2024, 13, 1495−1502

Building tunable degradation into high-performance poly (acrylate) pressure-sensitive adhesives. *ACS Macro Lett.* **2023**, *12* (6), 787−793.
(38) Choi, C.; Okayama, Y.; Morris, P. T.; Robinson, L. L.; Gerst, M.; Speros, J. C.; Hawker, C. J.; Read de Alaniz, J.; Bates, C. M. Digital light processing of dynamic bottlebrush materials. *Adv. Funct. Mater.* **2022**, *32* (25), 2200883.
(39) Zhu, G.; von Coelln, N.; Hou, Y.; Vazquez-Martel, C.; Spiegel, C. A.; Tegeder, P.; Blasco, E. Digital Light 3D Printing of Double Thermoplastics with Customizable Mechanical Properties and Versatile Reprocessability. *Adv. Mater.* **2024**, *36*, 2401561.
(40) Machado, T. O.; Stubbs, C. J.; Chiaradia, V.; Alraddadi, M. A.; Brandolese, A.; Worch, J. C.; Dove, A. P. A renewably sourced, circular photopolymer resin for additive manufacturing. *Nature* **2024**, *629*, 1069−1074.
(41) Stansbury, J. W.; Idacavage, M. J. 3D printing with polymers: Challenges among expanding options and opportunities. *Dental Mater.* **2016**, *32* (1), 54−64.
(42) Lee, T. Y.; Roper, T. M.; Jonsson, E. S.; Kudyakov, I.; Viswanathan, K.; Nason, C.; Guymon, C.; Hoyle, C. E. The kinetics of vinyl acrylate photopolymerization. *Polymer* **2003**, *44* (10), 2859−2865.
(43) Matyjaszewski, K.; Davis, T. P. *Handbook of Radical Polymerization*; Wiley Online Library, 2002.
(44) Voet, V. S.; Guit, J.; Loos, K. Sustainable photopolymers in 3D printing: a review on biobased, biodegradable, and recyclable alternatives. *Macro. Rapid Commun.* **2021**, *42* (3), 2000475.
(45) Rade, P.; Swami, S.; Pawane, V.; Hawaldar, R.; Giramkar, V.; Joseph, S.; Kale, B. Effect of functionality of diluents on digital light processing (DLP) based three-dimensional (3D) printing of UV-curable bisphenol A-based epoxy acrylate resin. *Polym. Eng. Sci.* **2024**, *64* (5), 2202−2213.
(46) Ghosh, A.; Kozlowski, K.; Steele, T. W. Synthesis and Evaluation of Metal Lipoate Adhesives. *Polymers* **2023**, *15* (13), 2921.
(47) Fan, Y.; Wang, X.; Zhang, X.; Chang, Z.; Kuang, W.; Tian, H. Recyclable Ionic Conductive Hydrogels Based on Autonomous Polymerization of α-Lipoic Acid for Flexible Wearable Electronic Sensors. *ACS Appl. Polym. Mater.* **2023**, *5* (10), 8430−8441.
(48) Islam, M. A.; Talukder, L.; Al, M. F.; Sarker, S. K.; Muyeen, S.; Das, P.; Hasan, M. M.; Das, S. K.; Islam, M. M.; Islam, M. R.; et al. A review on self-healing featured soft robotics. *Frontiers in Robotics and AI* **2023**, *10*, 1202584.
(49) Wang, X.; Zhao, M.; Zhang, L.; Li, K.; Wang, D.; Zhang, L.; Zhang, A.; Xu, Y. Liquid metal bionic instant self-healing flexible electronics with full recyclability and high reliability. *Chem. Eng. J.* **2022**, *431*, 133965.

https://doi.org/10.1021/acsmacrolett.4c00600
ACS Macro Lett. 2024, 13, 1495−1502